A Structural Dynamic Response Reconstruction Method for Continuous System Based on Kalman Filter

LI Hongqiu[1], *JIANG Jinhui*[2*], *MOHAMED M Shadi*[3]

1. School of Mechanical and Electrical Engineering, Jinling Institute of Technology, Nanjing 211169, P. R. China;
2. State Key Laboratory of Mechanics and Control for Aerospace Structures, Nanjing University of Aeronautics and Astronautics, Nanjing 210016, P. R. China;
3. Institute for Infrastructure and Environment, Heriot-Watt University, Edinburgh EH14 4AS, UK

(Received 18 November 2024; revised 3 March 2025; accepted 7 April 2025)

Abstract: The structural dynamic response reconstruction technology can extract unmeasured information from limited measured data, significantly impacting vibration control, load identification, parameter identification, fault diagnosis, and related fields. This paper proposes a dynamic response reconstruction method based on the Kalman filter, which simultaneously identifies external excitation and reconstructs dynamic responses at unmeasured positions. The weighted least squares method determines the load weighting matrix for excitation identification, while the minimum variance unbiased estimation determines the Kalman filter gain. The excitation prediction Kalman filter is constructed through time, excitation, and measurement updates. Subsequently, the response at the target point is reconstructed using the state vector, observation matrix, and excitation influence matrix obtained through the excitation prediction Kalman filter algorithm. An algorithm for reconstructing responses in continuous system using the excitation prediction Kalman filtering algorithm in modal space is derived. The proposed structural dynamic response reconstruction method evaluates the response reconstruction and the load identification performance under various load types and errors through simulation examples. Results demonstrate the accurate excitation identification under different load conditions and simultaneous reconstruction of target point responses, verifying the feasibility and reliability of the proposed method.

Key words: dynamic load identification; structural response reconstruction; excitation identification; Kalman filter; continuous system

CLC number: TB123 **Document code:** A **Article ID:** 1005-1120(2025)02-0250-11

0 Introduction

Dynamic loads can greatly affect the safety and stability of structures[1]. Obtaining dynamic load data, especially from hard-to-measure and critical points, is essential for research and structural health monitoring[2]. Structural dynamic response reconstruction technology can infer more unknown data from a limited number of measurement points, which to some extent compensates for the problem of insufficient measurement data[3]. Therefore, algorithms that can simultaneously identify structural dynamic loads and reconstruct responses are crucial.

For structural design and optimization, the precise knowledge of dynamic load on structures is essential. Jiang et al.[4] proposed a novel dynamic load identification method that took into account unknown initial conditions of structures which was based on the improved basis functions and the implicit Newmark-β method. Cui et al.[5] introduced a convolutional neural network (CNN) for the reconstruction of the interval of unknown load. Combining the interval analysis theory with the Taylor expansion, the upper and lower boundaries of the supervised loads are obtained and used as training samples. The trained CNN model can directly identifies

*Corresponding author, E-mail address: jiangjinhui@nuaa.edu.cn.

How to cite this article: LI Hongqiu, JIANG Jinhui, MOHAMED M Shadi. A structural dynamic response reconstruction method for continuous system based on Kalman filter[J]. Transactions of Nanjing University of Aeronautics and Astronautics, 2025, 42(2): 250-260.

http://dx.doi.org/10.16356/j.1005-1120.2025.02.009

the boundaries of the unknown load interval. Yang et al.[6] proposed a new method for dynamic load identification based on deep dilated convolutional neural network (DCNN), which directly constructed the inverse model between vibration response and excitation, avoiding solving model parameters. This method is based on Kalman filtering and is used to reconstruct the dynamic response of uncertain structures in linear systems. Using classical Kalman filtering to process uncertain models requires obtaining specific excitation information. Li et al.[7] introduced the extended Kalman filter(EKF) method combined with the least square estimation to identify the unknown load acting on the time-varying structure and realized the tracking of the structural parameters of the time-varying system. Aucejo et al.[8] explored the adaptability of the adaptive Kalman filter (AKF) in reconstructing mechanical sources, proposing a new state space representation of dynamic systems based on a generalized method. Under the augmented Kalman filter, using only the accelerometer signal may result in algorithm recognition divergence due to the unobservability and insufficient rank of the augmented matrix.

The method for reconstructing dynamic responses in uncertain structures within linear systems relies on Kalman filtering. While the classical Kalman filtering addresses uncertain models, obtaining specific excitation information is necessary. Li et al.[9] derived the motion equation in absolute coordinate system and then expanded the equation into modal space. In addition, the proposed method allows for identifying earthquake ground motion using incomplete modal information and limited measurements through the standard Kalman filter. Huang et al.[10] proposed two generalized algorithms based on the generalized Kalman filtering under unknown input (GKF-UI) for the identification of seismic ground excitation to multi-story and tall buildings, respectively. Naets et al.[11] utilized an improved augmented Kalman filter algorithm based on measurement to resolve prediction result divergence. Maes et al.[12] introduced a joint input state estimation (JISE) algorithm considering model-measurement error correlation and time delay, along with a smoothing algorithm based on JISE, applied to actual projects for practical measurements. Aucejo et al.[13] explored the adaptability of AKF in reconstructing mechanical sources, proposing a new state space representation of dynamic systems based on a generalized method.

The Kalman filtering algorithm shows promise in reconstructing structural dynamic responses, particularly in cases with model errors. However, the simultaneous reconstruction of structural external excitation and response has received limited attentions. Lei et al.[14] proposed a generalized Kalman filter with unknown input to identify structural states and unknown excitations in real-time. A revised version of observation equation is present by He et al.[15] for the simultaneous identification of structural parameters and the unknown excitations. Tang et al.[16] explored the influence of various filtering parameters (covariance matrix $\boldsymbol{Q}$ of model noise and covariance matrix $\boldsymbol{R}$ of measurement noise) in extended Kalman filtering on the time-varying parameter tracking performance of the structure.

The modal expansion technique is adopted to reduce the dimension of the motion equations and the size of the structural state to be identified[17-18]. These work above focused on the discrete system. On the basis of the classical Kalman filtering method, this paper proposes a Kalman filtering algorithm based on excitation prediction, used for the reconstruction of structural dynamic response for continuous systems. The Kalman filtering algorithm in modal space for continuous system is derived and investigated with modal parameters and noise disturbance.

Initially, the weighted least squares method is used to determine the load weighting matrix to identify the excitation, and the minimum variance unbiased estimation is used to determine the Kalman filter gain. The excitation prediction Kalman filter is constructed through time update, excitation update, and measurement update. Then, the calculation process of the excitation prediction Kalman filter algorithm is presented, extending the algorithm from physical space to mode space for continuous systems. Finally, a simple supported beam system is taken as a simulation example to analyze the feasibility and reliability of load identification and response reconstruction under different external excitations, such as impact excitation and fixed frequency excitation. Various noise conditions and model errors are introduced to evaluate the noise resistance of this method. The simulation results demonstrate that the algorithm can effectively identify and reconstruct various excitations.

1 Structural Dynamic Response Reconstruction Algorithm Based on Excitation Prediction Kalman Filter for Multi-degree of Freedom System

1.1 Response reconstruction algorithm in physical space

A study was conducted on the response reconstruction of multi-degree of freedom systems, and the response reconstruction process of multi-degree of freedom systems in physical space and modal space was derived. The model is shown in Fig.1, where m_i represents mass, k_i denotes stiffness, c_i is damping, $F_i(t)$ indicates the external dynamic load and p_i indicates the displacement, $i=1,2,\cdots,n$.

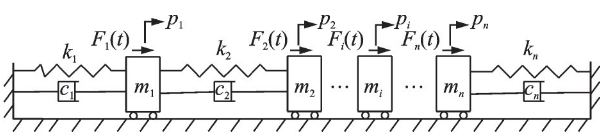

Fig.1 Multi-degree of freedom system under concentrated force

The motion equation of an n-degree-of-freedom dynamical system shown in Fig.1 is

$$\boldsymbol{M}\ddot{\boldsymbol{p}}(t)+\boldsymbol{C}\dot{\boldsymbol{p}}(t)+\boldsymbol{K}\boldsymbol{p}(t)=\boldsymbol{B}_u\boldsymbol{u}(t) \tag{1}$$

where $\boldsymbol{M}$, $\boldsymbol{C}$ and $\boldsymbol{K}$ represent the mass matrix, damping matrix and stiffness matrix, respectively; $\boldsymbol{p}(t)$, $\dot{\boldsymbol{p}}(t)$, and $\ddot{\boldsymbol{p}}(t)$ the displacement, velocity, and acceleration vectors, respectively; and $\boldsymbol{B}_u$ represents the influence matrix of the external load $\boldsymbol{u}(t)$, which is related to the position of the load. The matrix consists of 0 and 1, with all values being 0 except for 1 at the load location.

To transform the dynamic motion Eq.(1) into a linear state-space form, we have

$$\dot{\boldsymbol{x}}(t)=\boldsymbol{A}_c\boldsymbol{x}(t)+\boldsymbol{B}_c\boldsymbol{u}(t) \tag{2}$$

$$\boldsymbol{y}(t)=\boldsymbol{H}\boldsymbol{x}(t)+\boldsymbol{D}\boldsymbol{u}(t) \tag{3}$$

where

$$\begin{cases}\boldsymbol{x}(t)=\begin{bmatrix}\boldsymbol{p}(t)\\ \dot{\boldsymbol{p}}(t)\end{bmatrix}\\ \boldsymbol{A}_c=\begin{bmatrix}0 & \boldsymbol{I}\\ -\boldsymbol{M}^{-1}\boldsymbol{K} & -\boldsymbol{M}^{-1}\boldsymbol{C}\end{bmatrix}\\ \boldsymbol{B}_c=\begin{bmatrix}0\\ \boldsymbol{M}^{-1}\boldsymbol{B}_u\end{bmatrix}\end{cases} \tag{4}$$

And, $\boldsymbol{x}(t)$ and $\boldsymbol{y}(t)$ are the structure state vector and measurement vector, respectively; $\boldsymbol{A}_c$ and $\boldsymbol{B}_c$ the state transfer matrix and the excitation influence matrix; $\boldsymbol{H}$ and $\boldsymbol{D}$ the observation matrix and excitation influence matrix, respectively. When the measured value is acceleration, we have

$$\begin{cases}\boldsymbol{H}=[-\boldsymbol{H}_0\boldsymbol{M}^{-1}\boldsymbol{K} \quad -\boldsymbol{H}_0\boldsymbol{M}^{-1}\boldsymbol{C}]\\ \boldsymbol{D}=\boldsymbol{H}_0\boldsymbol{M}^{-1}\boldsymbol{B}_u\end{cases} \tag{5}$$

Assuming the equispaced sampling time instant is $t(t=t_0,t_1,\cdots,t_k)$ and these instants are small enough, we can also reasonably assume that the excitation $\boldsymbol{u}(t)$ remains unchanged within $\Delta t=t_{k+1}-t_k$, and Eqs.(2) and (3) can be discretized as

$$\begin{cases}\boldsymbol{x}_{k+1}=\boldsymbol{A}\boldsymbol{x}_k+\boldsymbol{B}\boldsymbol{u}_k\\ \boldsymbol{y}_k=\boldsymbol{H}\boldsymbol{x}_k+\boldsymbol{D}\boldsymbol{u}_k\end{cases} \tag{6}$$

where $\boldsymbol{u}_k$ is the external excitation; $\boldsymbol{x}_{k+1}$ and $\boldsymbol{x}_k$ represent the structural state vectors at time $(k+1)\Delta t$ and $k\Delta t$, respectively; $\boldsymbol{A}$ and $\boldsymbol{B}$ the state transition matrix and the excitation influence matrix in a discrete format, respectively, and defined as

$$\boldsymbol{A}=\mathrm{e}^{\boldsymbol{A}_c\Delta t} \tag{7}$$

$$\boldsymbol{B}=\int_0^{\Delta t}\boldsymbol{A}(0,\tau)\boldsymbol{B}_c\mathrm{d}\tau=\int_0^{\Delta t}\mathrm{e}^{\boldsymbol{A}_c\tau}\boldsymbol{B}_c\mathrm{d}\tau=\int_0^{\Delta t}\mathrm{e}^{\boldsymbol{A}_c\tau}\mathrm{d}\tau\boldsymbol{B}_c=(\boldsymbol{A}-\boldsymbol{I})\boldsymbol{A}_c^{-1}\boldsymbol{B}_c \tag{8}$$

1.2 Response reconstruction of Kalman filter based on excitation prediction

A structural dynamic response reconstruction method based on the excitation prediction Kalman filter is proposed, which includes an excitation identification step and uses weighted least squares to identify the excitation. Combining Kalman filtering for state estimation and utilizing time update steps and measurement update steps to achieve recursion and state correction, can simultaneously achieve excitation recognition and response reconstruction.

The specific calculation process is as follows.

(1) Time update step

According to Eq.(6), we get

$$\boldsymbol{x}_{k|(k-1)}=\boldsymbol{A}\boldsymbol{x}_{(k-1)|(k-1)}+\boldsymbol{B}\hat{\boldsymbol{u}}_{k-1} \tag{9}$$

where $\boldsymbol{x}_{k|(k-1)}$ is a priori estimate, and $\boldsymbol{x}_{(k-1)|(k-1)}$ a posteriori estimate of time $k-1$.

The error of the estimate of $\boldsymbol{x}_{k|(k-1)}$ is

$$\tilde{\boldsymbol{x}}_{k|(k-1)}\equiv\boldsymbol{x}_k-\boldsymbol{x}_{k|(k-1)}=\boldsymbol{A}\tilde{\boldsymbol{x}}_{(k-1)|(k-1)}+\boldsymbol{B}\tilde{\boldsymbol{u}}_{k-1}+\boldsymbol{w}_{k-1} \tag{10}$$

where $\tilde{\boldsymbol{x}}_{k|k}\equiv\boldsymbol{x}_k-\boldsymbol{x}_{k|k}$, and $\boldsymbol{w}_{k-1}$ is considered to be independent identically distributed Gaussian noise with the mean value 0.

(2) Excitation identification step

Define residuals as

$$\tilde{\boldsymbol{y}}_k\equiv\boldsymbol{y}_k-\boldsymbol{H}\boldsymbol{x}_{k|(k-1)} \tag{11}$$

$$\boldsymbol{y}_k=\boldsymbol{H}\boldsymbol{x}_k+\boldsymbol{D}\boldsymbol{u}_k+\boldsymbol{v}_k \tag{12}$$

where $\boldsymbol{v}_k$ represents the measurement error.

Get the relationship between $\tilde{\boldsymbol{y}}_k$ and $\boldsymbol{u}_k$, shown as

$$\tilde{\boldsymbol{y}}_k=\boldsymbol{D}\boldsymbol{u}_k+\boldsymbol{H}\tilde{\boldsymbol{x}}_{k|(k-1)}+\boldsymbol{v}_k=\boldsymbol{D}\boldsymbol{u}_k+\boldsymbol{e}_k \tag{13}$$

where $\boldsymbol{e}_k=\boldsymbol{H}\tilde{\boldsymbol{x}}_{k|(k-1)}+\boldsymbol{v}_k$. Since $\boldsymbol{x}_{k|(k-1)}$ is an unbiased estimation and $E(\boldsymbol{v}_k)=0$, we can obtain $E(\tilde{\boldsymbol{y}}_k)=\boldsymbol{D}E(\boldsymbol{u}_k)$. Next, the external excitation is estimated as

$$\hat{\boldsymbol{u}}_k=\boldsymbol{J}_k(\boldsymbol{y}_k-\boldsymbol{H}\boldsymbol{x}_{k|(k-1)}) \tag{14}$$

where $\boldsymbol{J}_k$ is to be a solved parameter which makes $\hat{\boldsymbol{u}}_k$ be an unbiased estimation of the external excitation $\boldsymbol{u}_k$.

Replacing Eq.(14) with Eq.(12), we obtain

$$\hat{\boldsymbol{u}}_k=\boldsymbol{J}_k\boldsymbol{D}\boldsymbol{u}_k+\boldsymbol{J}_k\boldsymbol{e}_k \tag{15}$$

If $\hat{\boldsymbol{u}}_k$ is an unbiased estimate of $\boldsymbol{u}_k$, we have $\boldsymbol{J}_k\boldsymbol{D}=\boldsymbol{I}$. Let

$$\tilde{\boldsymbol{R}}_k\equiv E(\boldsymbol{e}_k\boldsymbol{e}_k^{\mathrm{T}})=\boldsymbol{H}\boldsymbol{P}_{k|(k-1)}^{x}\boldsymbol{H}^{\mathrm{T}}+\boldsymbol{R}_k \tag{16}$$

where $\boldsymbol{R}_k\equiv E(\boldsymbol{v}_k\boldsymbol{v}_k^{\mathrm{T}})$, and $\tilde{\boldsymbol{R}}_k$ is a positive definite matrix. According to the least squares method, it can be inferred that

$$\boldsymbol{J}_k=(\boldsymbol{D}^{\mathrm{T}}\tilde{\boldsymbol{R}}_k^{-1}\boldsymbol{D})^{-1}\boldsymbol{D}^{\mathrm{T}}\tilde{\boldsymbol{R}}_k^{-1} \tag{17}$$

Predicting $\boldsymbol{u}_k$ is also a parameter estimation method similar to weighted least squares. Let $\tilde{\boldsymbol{y}}_k$ be the observation value and $\tilde{\boldsymbol{R}}_k^{-1}$ be the weight, then the variance $\boldsymbol{P}_k^{u}$ of $\tilde{\boldsymbol{u}}_k$ is

$$\begin{aligned}\boldsymbol{P}_k^{u}&=E(\tilde{\boldsymbol{u}}_k\tilde{\boldsymbol{u}}_k^{\mathrm{T}})=\boldsymbol{J}_k\boldsymbol{e}_k\boldsymbol{e}_k^{\mathrm{T}}\boldsymbol{J}_k^{\mathrm{T}}=\\&\boldsymbol{J}_k(\boldsymbol{H}\tilde{\boldsymbol{x}}_{k|(k-1)}+\boldsymbol{v}_k)(\boldsymbol{H}\tilde{\boldsymbol{x}}_{k|(k-1)}+\boldsymbol{v}_k)^{\mathrm{T}}\boldsymbol{J}_k^{\mathrm{T}}=\\&\boldsymbol{J}_k(\boldsymbol{H}\boldsymbol{P}_{k|(k-1)}^{x}\boldsymbol{H}^{\mathrm{T}}+\boldsymbol{R}_k)\boldsymbol{J}_k=\\&(\boldsymbol{D}^{\mathrm{T}}\tilde{\boldsymbol{R}}_k^{-1}\boldsymbol{D})^{-1}\boldsymbol{D}^{\mathrm{T}}\tilde{\boldsymbol{R}}_k^{-1}\tilde{\boldsymbol{R}}_k\tilde{\boldsymbol{R}}_k^{-1}\boldsymbol{D}[(\boldsymbol{D}^{\mathrm{T}}\tilde{\boldsymbol{R}}_k^{-1}\boldsymbol{D})^{-1}]^{\mathrm{T}}=\\&(\boldsymbol{D}^{\mathrm{T}}\tilde{\boldsymbol{R}}_k^{-1}\boldsymbol{D})^{-1}\end{aligned} \tag{18}$$

(3) Measurement update step

For measurement update, we assume that

$$\boldsymbol{x}_{k|k}=\boldsymbol{x}_{k|(k-1)}+\boldsymbol{K}_k(\boldsymbol{y}_k-\boldsymbol{H}\boldsymbol{x}_{k|(k-1)}-\boldsymbol{D}\hat{\boldsymbol{u}}_k) \tag{19}$$

where $\boldsymbol{K}_k$ is the Kalman gain, which can be solved by minimizing the variance matrix using the weighted least squares method[19].

$$\boldsymbol{K}_k=\boldsymbol{P}_{k|(k-1)}^{x}\boldsymbol{H}^{\mathrm{T}}\tilde{\boldsymbol{R}}_k^{-1} \tag{20}$$

$$\boldsymbol{P}_{k|k}^{x}=\boldsymbol{P}_{k|(k-1)}^{x}-\boldsymbol{K}_k(\tilde{\boldsymbol{R}}_k^{-1}-\boldsymbol{D}\boldsymbol{P}_k^{u}\boldsymbol{D}^{\mathrm{T}})\boldsymbol{K}_k^{\mathrm{T}} \tag{21}$$

So far, the derivation of the Kalman filter algorithm based on excitation prediction has been completed. The time update step, force identification step, and measurement update step are detailed below

$$\begin{cases}\boldsymbol{x}_{k|(k-1)}=\boldsymbol{A}\boldsymbol{x}_{(k-1)|(k-1)}+\boldsymbol{B}\hat{\boldsymbol{u}}_{k-1}\\\hat{\boldsymbol{u}}_k=\boldsymbol{J}_k(\boldsymbol{y}_k-\boldsymbol{H}\boldsymbol{x}_{k|(k-1)})\\\boldsymbol{x}_{k|k}=\boldsymbol{x}_{k|(k-1)}+\boldsymbol{K}_k(\boldsymbol{y}_k-\boldsymbol{H}\boldsymbol{x}_{k|(k-1)}-\boldsymbol{D}\hat{\boldsymbol{u}}_k)\end{cases} \tag{22}$$

To sum up, the flow of Kalman filter algorithm based on excitation prediction is given in Table 1.

Table 1 Kalman filter algorithm based on excitation prediction

(1) Given the initial values $\boldsymbol{x}_{0|-1}$, $\boldsymbol{P}_{0|-1}^{x}$
(2) Exciation identification step
$\tilde{\boldsymbol{R}}_k=\boldsymbol{H}\boldsymbol{P}_{k|(k-1)}^{x}\boldsymbol{H}^{\mathrm{T}}+\boldsymbol{R}_k$
$\boldsymbol{J}_k=(\boldsymbol{D}^{\mathrm{T}}\tilde{\boldsymbol{R}}_k^{-1}\boldsymbol{D})^{-1}\boldsymbol{D}^{\mathrm{T}}\tilde{\boldsymbol{R}}_k^{-1}$
$\hat{\boldsymbol{u}}_k=\boldsymbol{J}_k(\boldsymbol{y}_k-\boldsymbol{H}\boldsymbol{x}_{k|(k-1)})$
$\boldsymbol{P}_k^{u}=(\boldsymbol{D}^{\mathrm{T}}\tilde{\boldsymbol{R}}_k^{-1}\boldsymbol{D})^{-1}$
(3) Measurement update step
$\boldsymbol{K}_k=\boldsymbol{P}_{k|(k-1)}^{x}\boldsymbol{H}^{\mathrm{T}}\tilde{\boldsymbol{R}}_k^{-1}$
$\boldsymbol{x}_{k|k}=\boldsymbol{x}_{k|(k-1)}+\boldsymbol{K}_k(\boldsymbol{y}_k-\boldsymbol{H}\boldsymbol{x}_{k|(k-1)}-\boldsymbol{D}\hat{\boldsymbol{u}}_k)$
$\boldsymbol{P}_{k|k}^{x}=\boldsymbol{P}_{k|(k-1)}^{x}-\boldsymbol{K}_k(\tilde{\boldsymbol{R}}_k^{-1}-\boldsymbol{D}\boldsymbol{P}_k^{u}\boldsymbol{D}^{\mathrm{T}})\boldsymbol{K}_k^{\mathrm{T}}$
$\boldsymbol{P}_k^{xu}=(\boldsymbol{P}_k^{ux})^{\mathrm{T}}=\boldsymbol{K}_k\boldsymbol{D}\boldsymbol{P}_k^{u}$
(4) Time update step
$\boldsymbol{x}_{(k+1)|k}=\boldsymbol{A}\boldsymbol{x}_{k|k}+\boldsymbol{B}\hat{\boldsymbol{u}}_k$
$\boldsymbol{P}_{(k+1)|k}^{x}=[\boldsymbol{A}\quad\boldsymbol{B}]\begin{bmatrix}\boldsymbol{P}_{k|k}^{x}&\boldsymbol{P}_k^{xu}\\\boldsymbol{P}_k^{ux}&\boldsymbol{P}_k^{u}\end{bmatrix}\begin{bmatrix}\boldsymbol{A}^{\mathrm{T}}\\\boldsymbol{B}^{\mathrm{T}}\end{bmatrix}+\boldsymbol{G}_k$

In order to achieve structural response reconstruction, which involves using signals from a limited number of observation points to predict the response values of the target point, we utilize a Kalman filter algorithm based on excitation prediction, as described earlier. This enables us to obtain system state and excitation predictions, thereby facilitating structural response reconstruction. At this point, the state transition equation and observation equation can be expressed as follows

$$\begin{cases} \boldsymbol{x}_k = \boldsymbol{A}\boldsymbol{x}_{k-1} + \boldsymbol{B}\boldsymbol{u}_{k-1} + \boldsymbol{w}_{k-1} \\ \boldsymbol{y}_k^{\mathrm{m}} = \boldsymbol{H}^{\mathrm{m}}\boldsymbol{x}_k + \boldsymbol{D}^{\mathrm{m}}\boldsymbol{u}_k + \boldsymbol{v}_k \end{cases} \tag{23}$$

where the superscript m denotes the measurement position, signifying the position of the measured value. In accordance with Eq.(23), the reconstruction response at the target point can be obtained through Kalman filtering, representing the posterior value $\boldsymbol{x}_{k|k}$

$$\boldsymbol{y}_k^{\mathrm{r}} = \boldsymbol{H}^{\mathrm{r}}\boldsymbol{x}_{k|k} + \boldsymbol{D}^{\mathrm{r}}\hat{\boldsymbol{u}}_k \tag{24}$$

where the superscript r indicates the position of the reconstruction value of the target point, and $\boldsymbol{y}_k^{\mathrm{r}}$ the response value of the reconstruction of the target point. Now, if $\boldsymbol{y}_k$ is taken as the true response value of the target point, then

$$\boldsymbol{y}_k = \boldsymbol{H}^{\mathrm{r}}\boldsymbol{x}_k + \boldsymbol{D}^{\mathrm{r}}\hat{\boldsymbol{u}}_k \tag{25}$$

When applying this algorithm to reconstruct the dynamic response of a known structure under unknown excitation, the model parameters of the structure must be calculated as algorithm parameters. In addition, the response data collected from finite element simulations or sensors should be input as observations into the algorithm. This process can perform dynamic response reconstruction (DRR) of the structure and predict excitation. Although the measurement signals in this article are exclusive acceleration ones, this response reconstruction method is still feasible for other measurement signals such as strain, displacement, and velocity.

2 Response Reconstruction Algorithm of Multi-degree Freedom System in Modal Space

In physical space, a large number of multi degree of freedom systems involve complex parameter matrices such as $\boldsymbol{A}_c$, $\boldsymbol{B}_c$. During response reconstruction operations based on Kalman filtering, the recursive process greatly increases the operating pressure on the computer, and in many cases, it is even impossible to obtain them. In actual system vibration, the first few modes often play a dominant role. These modes contribute significantly to the vibration of the system. Therefore, consider performing modal transformation on it in the modal space, which is, using the first few dominant modes to reasonably replace the entire system mode. In this paper, the number of modal truncation is 4.

To reconstruct the dynamic response of a structure in modal space, it is first necessary to decouple the vibration differential equation and transform it from physical space to modal space. According to the modal analysis theory, the displacement of a structure can be obtained through modal transformation, shown as

$$\boldsymbol{p}(t) = \boldsymbol{\Phi}\boldsymbol{q}(t) \tag{26}$$

where $\boldsymbol{q}(t)$ is the modal displacement vector, and $\boldsymbol{\Phi}$ the modal mode shape matrix of the system.

For $|[\boldsymbol{K}] - \omega_n^2[\boldsymbol{M}]| = 0$, the natural frequency and mode vector of the system are $\omega_1, \omega_2, \cdots, \omega_n$ and $\boldsymbol{\Phi} = [\varphi_1 \ \ \varphi_2 \ \ \cdots \ \ \varphi_n]$, respectively.

Substituting Eq.(26) into Eq.(1), the motion equation of the dynamic system can be written as

$$\boldsymbol{\Phi}^{\mathrm{T}}\boldsymbol{M}\boldsymbol{\Phi}\ddot{\boldsymbol{q}}(t) + \boldsymbol{\Phi}^{\mathrm{T}}\boldsymbol{C}\boldsymbol{\Phi}\dot{\boldsymbol{q}}(t) + \boldsymbol{\Phi}^{\mathrm{T}}\boldsymbol{K}\boldsymbol{\Phi}\boldsymbol{q}(t) = \boldsymbol{\Phi}^{\mathrm{T}}\boldsymbol{B}_u\boldsymbol{u}(t) \tag{27}$$

with $\boldsymbol{u}(t) = [F_1(t) \ \ F_2(t) \ \ \cdots \ \ F_n(t)]$. If it meets

$$\boldsymbol{\Phi}^{\mathrm{T}}\boldsymbol{M}\boldsymbol{\Phi} = \boldsymbol{I} \tag{28}$$

$$\boldsymbol{\Phi}^{\mathrm{T}}\boldsymbol{K}\boldsymbol{\Phi} = \boldsymbol{\Lambda} \tag{29}$$

where $\boldsymbol{\Lambda} = \mathrm{diag}(\lambda_1 \ \ \lambda_2 \ \ \cdots \ \ \lambda_n)$ and $\lambda_i = \omega_i^2$ $(i=1, 2, \cdots, n)$, Eq.(27) can be abbreviated as

$$\ddot{\boldsymbol{q}}(t) + \boldsymbol{\Gamma}\dot{\boldsymbol{q}}(t) + \boldsymbol{\Lambda}\boldsymbol{q}(t) = \boldsymbol{\Phi}^{\mathrm{T}}\boldsymbol{B}_u\boldsymbol{u}(t) \tag{30}$$

where $\boldsymbol{\Gamma} = \boldsymbol{\Phi}^{\mathrm{T}}\boldsymbol{C}\boldsymbol{\Phi}$ represents the modal damping. If the system damping is proportional, the modal damping matrix $\boldsymbol{\Gamma}$ is

$$\boldsymbol{\Gamma} = \begin{bmatrix} 2\xi_1\omega_1 & 0 & \cdots & 0 \\ 0 & 2\xi_2\omega_2 & \cdots & 0 \\ \vdots & \vdots & & \vdots \\ 0 & 0 & \cdots & 2\xi_r\omega_r \end{bmatrix} \tag{31}$$

where $\gamma_i = 2\xi_i\omega_i$ represents the ith order modal damping, and ξ_i the ith order modal damping rate. Utilizing the modal analysis theory, Eq.(27) can also be converted into the state-space (Eq.(2)). Consequently, we have

$$\boldsymbol{x}(t) = \begin{bmatrix} \boldsymbol{q}(t) \\ \dot{\boldsymbol{q}}(t) \end{bmatrix}, \boldsymbol{A}_c = \begin{bmatrix} 0 & \boldsymbol{I} \\ -\boldsymbol{\Lambda} & -\boldsymbol{\Gamma} \end{bmatrix}, \boldsymbol{B}_c = \begin{bmatrix} 0 \\ \boldsymbol{\Phi}^{\mathrm{T}}\boldsymbol{B}_u \end{bmatrix} \tag{32}$$

Based on Eqs.(2—5), the discrete state-space equation and observation equation can be obtained. When the observation corresponds to acceleration signals, in modal space, we have $H = [-H_0 \boldsymbol{\Phi}\boldsymbol{\Phi}^{\mathrm{T}} K \quad -H_0 \boldsymbol{\Phi}\boldsymbol{\Phi}^{\mathrm{T}} C]$ and $D = H_0 \boldsymbol{\Phi}\boldsymbol{\Phi}^{\mathrm{T}} B_u$, here H_0 is a position matrix composed of 0 and 1.

Taking A, B, H, and D as inputs, the structural dynamic response is reconstructed. Through the excitation recognition step, the external excitation estimate $\hat{\boldsymbol{u}}_k$ of the system is identified. At the same time, the state estimate $\boldsymbol{x}_{k|k}$ is obtained through the measurement update step and time update step. Based on the partial observation values y_k of the system response under the input external excitation, the response information $\boldsymbol{y}_k^{\mathrm{r}}$ of the target point can be reconstructed.

3 Response Reconstruction Algorithm of Continuous System in Modal Space

For continuous system, the natural frequency, mass-normalized natural mode shape, and damping matrix of the model are directly acquired via Patran & Nastran. Once the modal truncation number is determined, the matrices $\boldsymbol{\Phi}$, $\boldsymbol{\Lambda}$, $\boldsymbol{\Gamma}$ are calculated, and then the parameter matrices $\boldsymbol{A}_c$ and $\boldsymbol{B}_c$ for the structural dynamic response method are constructed. Discretizing it using the time interval Δt, we derive the state transition matrix $\boldsymbol{A}$ and excitation influence matrix $\boldsymbol{B}$. if the observation is an acceleration signal, we have

$$H = [-H_0 \boldsymbol{\Phi}\boldsymbol{\Phi}^{\mathrm{T}} K \quad -H_0 \boldsymbol{\Phi}\boldsymbol{\Phi}^{\mathrm{T}} C], D = H_0 \boldsymbol{\Phi}\boldsymbol{\Phi}^{\mathrm{T}} B_u.$$

To ensure matrix $\boldsymbol{D}$ with full rank[20], the acceleration observation points include the locations where excitation acts.

In modal space, the estimation of the external excitation of the system is obtained through the excitation identification step, which is similar to the analysis of multi-degree-of-freedom systems. Simultaneously, the response information at the target point can be reconstructed. Fig.2 shows the flow chart of response reconstruction method for continuous system in modal space.

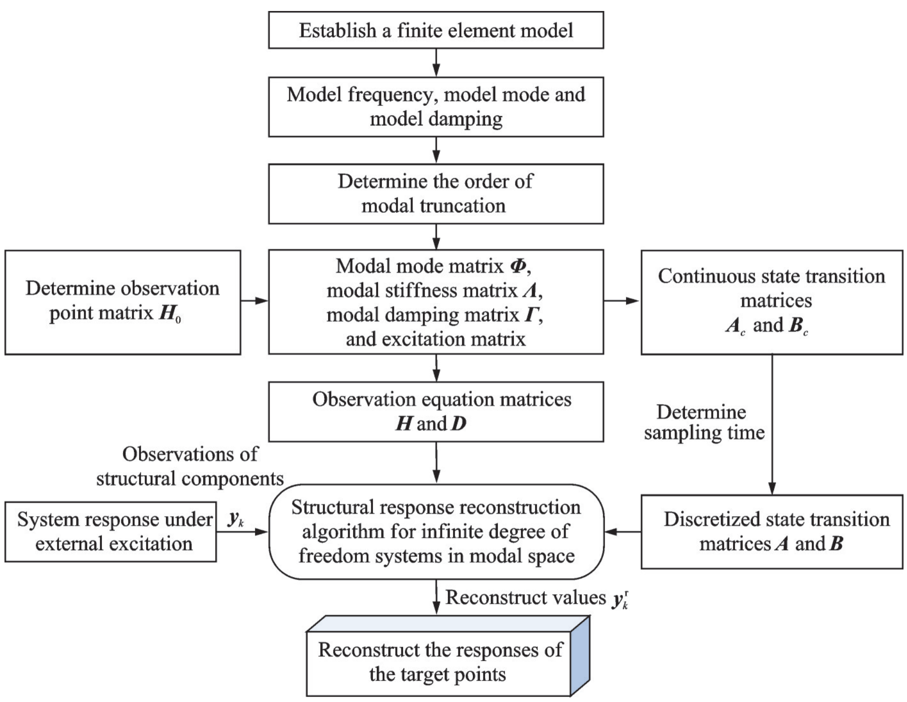

Fig.2　Flow chart of response reconstruction method for continuous system in modal space

4 Accuracy Evaluation Method

The peak relative error method (PREM), signal to noise ratio (SNR) and angle cosine method (ACM) are used to evaluate the accuracy of load identification. We assume that the theoretically accurate response signal is represented by $\boldsymbol{X}(i)$, while the reconstructed response signal is represented by $\boldsymbol{Y}(i)$.

(1) PREM

$$\mathrm{PREM}(\boldsymbol{X},\boldsymbol{Y})=\frac{|\max \boldsymbol{Y}(i)-\max \boldsymbol{X}(i)|}{\max \boldsymbol{X}(i)}\times 100\% \tag{33}$$

(2) SNR

$$\mathrm{SNR}(\boldsymbol{X},\boldsymbol{Y})=10\lg\left\{\frac{\sum_{i=1}^{n}\boldsymbol{X}^2(i)}{\sum_{i=1}^{n}\left[\boldsymbol{X}(i)-\boldsymbol{Y}(i)\right]^2}\right\} \tag{34}$$

(3) ACM

The similarity between two vectors can be measured by calculating the cosine of the angle θ between them, shown as

$$s(\boldsymbol{X},\boldsymbol{Y})=\cos\theta=\frac{\sum_{i=1}^{n}\boldsymbol{X}(i)\boldsymbol{Y}(i)}{\sqrt{\sum_{i=1}^{n}\boldsymbol{X}^2(i)\sum_{i=1}^{n}\boldsymbol{Y}^2(i)}} \tag{35}$$

5 Simulation Example

The simply supported beam model depicted in Fig.3 is taken as an example. The simply supported beam is 1 m long, 0.05 m wide, and 0.005 m thick. The elastic modulus is 206 GPa, the density is 7 900 kg/m^3, and the Poisson's ratio is 0.3. A dynamic load f is applied to the beam.

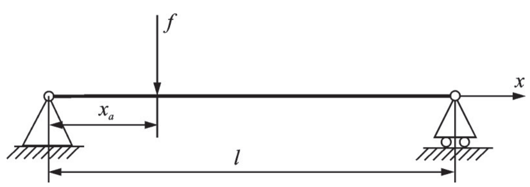

Fig.3 Simply supported beam under concentrated force

Following the dynamic response reconstruction method proposed in this paper for continuous system, the dynamic response of the target point is reconstructed using response information from a finite number of points. Simultaneously, the dynamic load applied to the structure is identified and compared with the actual structural dynamic response and load to verify the feasibility and accuracy of this dynamic response reconstruction method for a continuous structure.

5.1 Excitation identification and response reconstruction under impact excitation

For the simply supported beam model, the dynamic load is assumed to be an impact load and a half sine wave within a short duration, specifically from 0.1 s to 0.110 s, while the load remains 0 at other time. Let the dynamic load f defined as $f(t)=\sin(2\pi\times 50t)$.

The system begins in a zero initial state. The Patran software package is utilized for modelling the simply supported beam, while the Nastran software package is employed for transient dynamics analysis. The sampling time for acceleration response is 5 s, and the sampling rate is 1 024.

(1) Excitation identification and response reconstruction under error free impact excitation

When noise conditions are not taken into account, Fig.4 presents a partial enlarged view of the comparison results between the load identified in the excitation identification step and the actual value at the moment of force application. Similarly, Fig.5 depicts the comparison between the acceleration response of the target node reconstructed by the algorithm and the theoretical value. Table 2 presents the reconstruction error results under error free impact excitation, which are the average values obtained from multiple sets of data calculations.

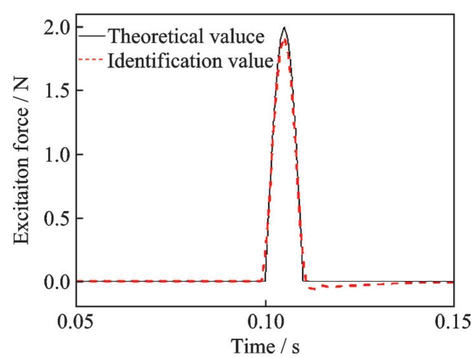

Fig.4 Partial magnification of identification results for error free impact excitation

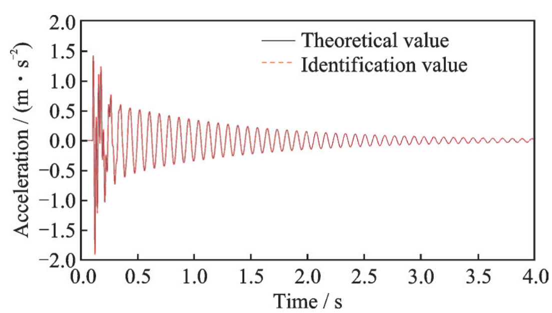

Fig.5 Reconstruction results of acceleration response of target nodes under error free impact excitation

Table 2 Reconstruction error results under error free impact excitation

Error evaluation method	PREM/ %	SNR/ dB	ACM
Load identification	3.99	37.9	0.99
Response reconstruction	0.44	98.8	1.00

From the above charts, it is evident that when noise is disregarded and accurate model parameters are employed, the structural dynamic response reconstruction algorithm effectively identifies impact excitation. Moreover, the reconstructed acceleration response signal, in terms of amplitude, SNR, and cosine value of the included angle, aligns perfectly with the theoretical value. Thus, the feasibility of excitation identification and response reconstruction using the algorithm proposed in this paper is confirmed under error-free conditions when applying impact loads.

(2) Excitation identification and response reconstruction under impact excitation considering modal parameter error and Gaussian white noise

Fig.6 provides a comparison between the identified excitation forces and the true applied loads at the moment of impact, considering 5% modal parameter errors and observation polluted with zero-mean Gaussian white noise (standard deviation 0.001). Similarly, Fig.7 demonstrates the consistency of the reconstructed acceleration response of the target node and its theoretical counterpart. Table 3 presents the reconstruction error results with 5% modal noise error and Gaussian white noise, which represent the average values computed from multiple data sets. As observed from Table 3, when Gaussian white noise and modal parameter noise are

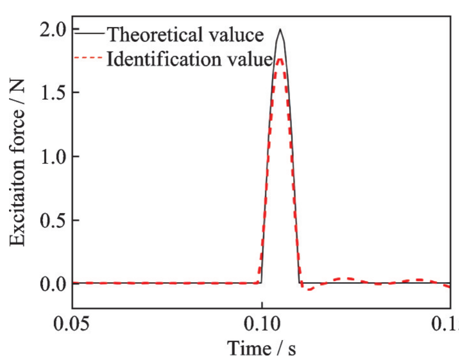

Fig.6 Partial magnification of identification results for impact excitation with 5% modal noise error and Gaussian white noise

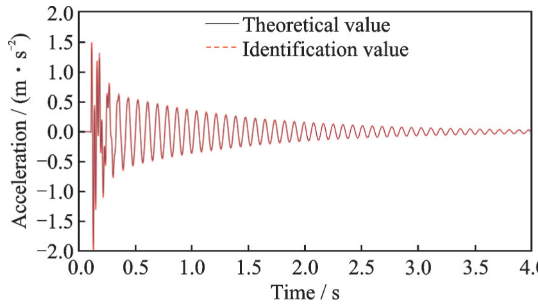

Fig.7 Reconstruction results of acceleration response of target nodes with 5% modal noise error and Gaussian white noise

Table 3 Reconstruction error results under impact excitation with 5% modal noise and Gaussian white noise

Error evaluation method	PREM/ %	SNR/ dB	ACM
Load identification	8.33	16.6	0.88
Response reconstruction	7.06	47.2	0.99

concurrently introduced, the relative error of the peak value remains within 10%. The SNR and the cosine value of the included angle are somewhat high, while they still fall within an acceptable error range for practical engineering applications. The maximum value of angle cosine method is 1, and the closer the value is to 1, the closer the recognition value or reconstruction value signal is to the theoretical value.

5.2 Excitation identification and response reconstruction under fixed frequency excitation

Let the dynamic load f be a fixed frequency load defined as $f(t)=\sin(2\pi\times 20t)+3\sin(2\pi\times 30t)$. Same as case one, Patran is utilized to simulate model for response calculation. With a sampling rate of 1 024 Hz, the sampling time is set to 5 s, and the acceleration response is computed accordingly. By combining the calculated response data with the natural frequencies and modes obtained through finite element analysis, we construct the parameter matrix required for the algorithm to reconstruct the response. The initial state vector of the system is assumed to be 0.

(1) Excitation identification and response reconstruction under error free fixed frequency excitation

When noise conditions are not taken into consideration, the model is analyzed accordingly. Following the algorithm, we compare the load identified by the excitation identification step with the actual value. Fig.8 and Fig.9 show the effectiveness of the identified excitation forces and reconstructed acceleration response, respectively, under fixed-frequency excitation conditions without model disturbance and noise interruption. Data results, which represent the average values computed from multiple data sets, are provided in Table 4.

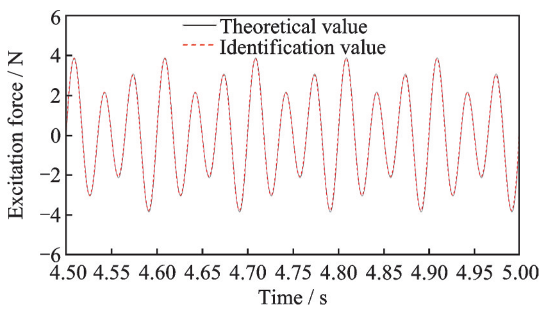

Fig.8 Partial amplification of identification results of fixed frequency excitation without error

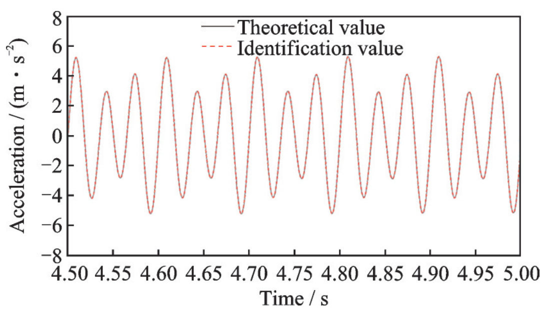

Fig.9 Partial magnification of reconstruction results of acceleration response without error

Table 4 Reconstruction error results without error when applying fixed frequency excitation

Error evaluation method	PREM/ %	SNR/ dB	ACM
Load identification	0.67	64.7	0.99
Response reconstruction	0.01	176.2	1.00

From the charts, it is evident that without considering noise and employing accurate model parameters, and when the applied force is a fixed frequency excitation, the algorithm can precisely identify the fixed frequency excitation. The relative error of its peak value is 0.67%, and the SNR and the cosine value of the included angle demonstrate an ideal overall degree of coincidence for the evaluation curve. Moreover, the response signal reconstructed by the algorithm perfectly aligns with the theoretical value in terms of amplitude, SNR, or cosine value of the included angle. This confirms the feasibility of load identification and response reconstruction when a fixed frequency excitation is applied without error.

(2) Excitation identification and response reconstruction under fixed frequency excitation considering modal parameter error and Gaussian white noise

Modal parameter errors and Gaussian white noise are factored to verify the algorithm. Assuming that the observation noise follows a Gaussian distribution with a mean of 0 and a standard deviation of 0.001, and incorporating a 5% modal parameter error, we assess the algorithm's performance. The comparisons between the identification or reconstructed result and theoretical value are presented in Fig.10 and Fig.11. As shown in figures, the good agreements can be obtained under the conditions of fixed-frequency excitation conditions with 5% model disturbance and zero-mean Gaussian white noise interruption (standard deviation 0.001). Data results, representing the average values calculated from multiple data sets, are provided in Table 5.

From the results, it is apparent that when considering the actual situation and introducing Gaussian white noise and modal parameter error, the relative error of the peak value remains within 10%. Fortunately, the SNR and the cosine value of the included angle result in an overall excellent identification and reconstruction effect. This validates the feasibility and reliability of the algorithm when a fixed

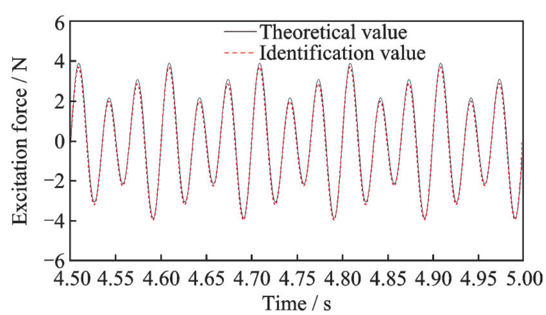

Fig.10 Partial amplification of identification results of fixed frequency excitation with 5% modal noise error and Gaussian white noise

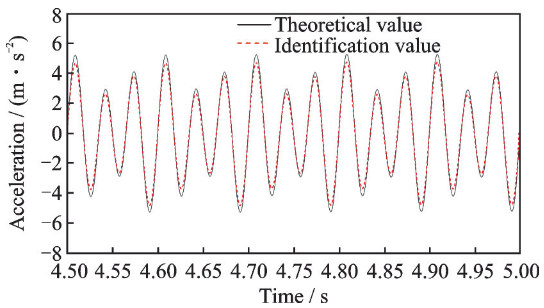

Fig.11 Partial amplification of reconstruction results of acceleration response of target node with 5% modal noise error and Gaussian white noise

Table 5 Reconstruction error results under fixed frequency excitation with 5% modal noise and Gaussian white noise

Error evaluation method	PREM/%	SNR/dB	ACM
Load identification	5.89	58.4	0.999
Response reconstruction	7.93	51.5	1.000

frequency excitation is applied to continuous system in a practical scenario.

6 Conclusions

A response reconstruction method based on excitation prediction Kalman filter was proposed, and the Kalman method based on excitation prediction was derived. The response reconstruction method was also derived using acceleration response signals. Extending the algorithm from physical space to mode space for multi-degree freedom system and continuous system. A simply supported beam system is taken as a simulation example to analyze the feasibility and reliability of load identification and response reconstruction under different external excitations, such as impact excitation and fixed frequency excitation. Various noise conditions and model errors are introduced to evaluate the noise resistance of this method. The simulation results demonstrate that the algorithm can effectively identify the excitation and reconstruct various excitations.

References

[1] LI H N, GAO D W, YI T H. Research status and progress of civil engineering structural health monitoring system[J]. Progress in Mechanics, 2008, 38(2): 151-166.

[2] LI Y, LUO Y, WAN H P, et al. Identification of earthquake ground motion based on limited acceleration measurements of structure using Kalman filtering technique[J]. Structural Control and Health Monitoring, 2020, 27(1): e2464.

[3] LEI Y, JIANG Y, XU Z. Structural damage detection with limited input and output measurement signals[J]. Mechanical Systems and Signal Processing, 2012, 28: 229-243.

[4] JIANG J, CUI W, CHEN S, et al. A novel dynamic load identification method based on improved basis functions and implicit Newmark-β for continuous system with unknown initial conditions[J]. Mechanical Systems and Signal Processing, 2024, 208: 110987.

[5] CUI W, JIANG J, SUN H, et al. Data-driven load identification method of structures with uncertain parameters[J]. Acta Mechanica Sinica, 2023, 40(2): 523138.

[6] YANG H, JIANG J, CHEN G, et al. Dynamic load identification based on deep convolution neural network[J]. Mechanical Systems and Signal Processing, 2023, 185: 109757.

[7] LI Y L, JIANG J H, TANG H Z. Dynamic load identification for structures with variable stiffness based on extended Kalman filter[J]. Transactions of Nanjing University of Aeronautics and Astronautics, 2022, 39(S1): 16-22.

[8] AUCEJO M, DE SMET O, DEÜ J F. Practical issues on the applicability of Kalman filtering for reconstructing mechanical sources in structural dynamics[J]. Journal of Sound and Vibration, 2019, 442: 45-70.

[9] LI Y, LUO Y, WAN H P, et al. Identification of earthquake ground motion based on limited acceleration measurements of structure using Kalman filtering technique[J]. Structural Control and Health Monitoring, 2020, 27(1): e2464.

[10] HUANG J, LI X, ZHANG F, et al. Identification of joint structural state and earthquake input based on a generalized Kalman filter with unknown input[J]. Mechanical Systems and Signal Processing, 2021, 151: 107362.

[11] NAETS F, CUADRADO J, DESMET W. Stable force identification in structural dynamics using Kalman filtering and dummy-measurements[J]. Mechanical Systems and Signal Processing, 2015, 50: 235-248.

[12] MAES K, SMYTH A W, DE ROECK G, et al. Joint input-state estimation in structural dynamics[J]. Mechanical Systems and Signal Processing, 2016, 70: 445-466.

[13] AUCEJO M, DE SMET O, DEÜ J F. Practical issues on the applicability of Kalman filtering for reconstructing mechanical sources in structural dynamics[J]. Journal of Sound and Vibration, 2019, 442: 45-70.

[14] LEI Y, JIANG Y, XU Z. Structural damage detection with limited input and output measurement sig-

nals[J]. Mechanical Systems and Signal Processing, 2012, 28: 229-243.

[15] HE J, ZHANG X, XU B. Identification of structural parameters and unknown inputs based on revised observation equation: Approach and validation[J]. International Journal of Structural Stability and Dynamics, 2019, 19(12): 1950156.

[16] TANG Hongzhi, JIANG Jinhui. Research on tracking performance of extended Kalman filter for time varying parameters[J]. Journal of Nanjing University of Aeronautics & Astronautics, 2022, 54(2): 304-310. (in Chinese)

[17] HE J, DENG B, HUA X, et al. Joint estimation of multi-scale structural responses and unknown loadings based on modal Kalman filter without using collocated acceleration observations[J]. International Journal of Structural Stability and Dynamics, 2022, 22(11): 2250132.

[18] WU J, QI C, ZHANG F, et al. State-input system identification of tall buildings under unknown seismic excitations based on modal Kalman filter with unknown input[J]. Journal of Aerospace Engineering, 2021, 34(4): 04021040.

[19] CHEN J, LI J, YANG S, et al. Weighted optimization-based distributed Kalman filter for nonlinear target tracking in collaborative sensor networks[J]. IEEE Transactions on Cybernetics, 2017, 47(11): 3892-3905.

[20] HE J, QI M, TONG Z, et al. An improved extended Kalman filter for parameters and loads identification without collocated measurements[J]. Smart Structures and Systems: An International Journal, 2023, 31(2): 10.

Acknowledgements This work was supported by the National Natural Science Foundation of China (Nos. 12372066, U23B6009, 52171261), the Aeronautical Science Fund (No.20240013052002), and the Qing Lan Project.

Authors

The first author Dr. **LI Hongqiu** received the Ph.D. degree in mechanical engineering from Nanjing University of Aeronautics and Astronautics, Nanjing, China, in 2011. From Nov. 2016 to Nov. 2017, she worked as a visiting scholar in School of Computer Science and Engineering, Durham University, UK. From 2011 to present, she has been with School of Mechanical and Electrical Engineering, Jinling Institute of Technology. Her research mainly focuses on dynamic load identification, vibration and noise control, finite element analysis and simulation.

The corresponding author Prof. **JIANG Jinhui** received the Ph.D. degree in engineering mechanics from Nanjing University of Aeronautics and Astronautics, Nanjing, China, in 2010. In July 2010, he joined Nanjing University of Aeronautics and Astronautics, Nanjing, China. From Jul. 2016 to Jul.2017, he worked as a visiting scholar in Durham University, UK. His research mainly focuses on structural dynamic load identification, vibration testing and data processing, etc.

Author contributions Dr. **LI Hongqiu** designed the study, conducted the analysis, interpreted the results and wrote the manuscript. Prof. **JIANG Jinhui** contributed to data and model components for the simulation. Dr. **MOHAMED M Shadi** provided important guidance in solving difficult or complex problems in the article. All authors commented on the manuscript draft and approved the submission.

Competing interests The authors declare no competing interests.

(Production Editor: ZHANG Huangqun)

基于卡尔曼滤波的连续系统结构动响应重构方法

李鸿秋[1],姜金辉[2],MOHAMED M Shadi[3]

(1.金陵科技学院机电工程学院,南京 211169,中国; 2.南京航空航天大学航空航天结构力学及控制全国重点实验室,南京 210016,中国; 3.赫瑞-瓦特大学基础设施与环境研究所,爱丁堡 EH14 4AS,英国)

摘要:从有限的测量数据中重构未测量位置的结构动响应信息,对振动控制、载荷识别、参数识别和故障诊断等领域具有重要意义。本文提出了一种基于卡尔曼滤波器的动态响应重建方法,该方法在识别外部激励的同时重建未测量位置的动态响应。采用加权最小二乘法确定载荷加权矩阵来识别激励,利用最小方差无偏估计确定卡尔曼滤波器增益。通过时间、激励和测量更新构建激励预测卡尔曼滤波,基于激励预测卡尔曼滤波算法获得的状态向量、观测矩阵和激励影响矩阵用于重建目标点处的响应,并推导了一种在模态空间中使用激励预测卡尔曼滤波重建连续系统响应的算法。仿真算例验证了不同载荷类型和误差下的响应重建和载荷识别效果。结果表明,在不同载荷工况条件下,所提出的算法能够准确辨识激励和重构目标点动响应,证明了该算法的可行性和可靠性。

关键词:动载荷识别;结构响应重建;激励识别;卡尔曼滤波器;连续系统